PERGAMON

Available online at www.sciencedirect.com

SCIENCE DIRECT®

International Journal of Heat and Mass Transfer 46 (2003) 4925–4934

International Journal of HEAT and MASS TRANSFER

www.elsevier.com/locate/ijhmt

Study of free convective heat transfer from horizontal conic

W.M. Lewandowski *, S. Leble

Department of Apparatus and Chemical Machinery, Gdańsk University of Technology, ul. G. Narutowicza 11/12, 80-952 Gdańsk, Poland

Received 4 February 2003

Abstract

Theoretical and experimental considerations of free convective heat transfer from horizontal isothermal conic in unlimited space are presented. In the theoretical part of the paper we introduced the curvilinear coordinate system compatible with conical surface and gravity field. The equations of Navier–Stokes and Fourier–Kirchhoff were simplified in this local orthogonal system. The resulting equation have been solved by asymptotic series in the vicinity of horizontal element of the cone. The final Nusselt–Rayleigh relation as a function of the conic base angle was verified experimentally. The experimental study was performed in water and air for conics with the angles equal to $\alpha = 0$ (vertical round plate), 30°, 45° and 60° and diameter of the base $D = 0.1$ m. The experimental results are in a good accordance (maximum within +8.7%) with the theory.

1. Introduction

The results of theoretical and experimental study of free convective heat transfer from conical surfaces were published and they are very useful to determine convective heat losses from conical fragments of apparatus in industrial or energetic installations, electronic equipment, architectonic objects and so on by engineers and designers. Unfortunately available dates are not complete. There are some information on vertical faced down or up cones [1–6] but for the horizontal ones we have found the only paper, written by Oosthuizen [7]. In the Churchill's review paper [8] among about 120 results devoted to free convection four positions are concerned conical (only vertical) surfaces. Oosthuizen's paper deal only with the experimental study.

Hence the paper presents theoretical solution of the natural convective heat transfer problem from the isothermal surface of a horizontal conic. We also show the experimental verification of the obtained analytical formulas. The experiments were performed in water and air for conics with the base angle: $\alpha = 0°$, 30°, 45° and 60°.

The phenomenon of convective fluid flow pattern for the configuration to be considered is complicated, because of the gravity field breaks the axis symmetry in comparison with vertical cones (Fig. 1a). In our first attempts we used of the cylindrical coordinate system successive in the case of horizontal cylinder (Fig. 1b) for the hypoeutectic stream line description (Fig. 1c). However, more profound study and the visualization (Fig. 2a) had been shown a failure of this first attempt.

This is the reason why we decided to introduce the special curvilinear coordinate system (ϵ, ϵ_m) based on the stream line curves S_i, shown in Fig. 2b and described in details together with continuous maps, transformations and final solution in papers [9,10]. We would like to stress that each curve S_i is not plain, by other words it is not conic. The variety of the curves cover the conic surface and parameterized by $\epsilon_m = \max(\epsilon)$.

2. The coordinate system and physical model

The isothermal lateral conic surface in Cartesian coordinates is described by the equation

* Corresponding author. Tel./fax: +48-58-347-24-10.
E-mail address: wlew@chem.pg.gda.pl (W.M. Lewandowski).

0017-9310/$ - see front matter © 2003 Elsevier Ltd. All rights reserved.
doi:10.1016/S0017-9310(03)00307-7

Nomenclature

a	thermal diffusivity (m^2/s)
a	function defined by Eq. (46)
A	control surface, Fig. 5 and Eq. (22) (m^2)
C	coefficient in Nusselt–Rayleigh relation Eq. (50) (dimensionless)
c_p	specific heat at constant pressure (J/(kg K))
D	diameter of the cone base (m)
dA_k	control surface of heated wall, Fig. 5 and Eq. (23) (m^2)
E	coefficient in Eq. (31)
$f = y''(0)$	coefficient in the Taylor expansion of $y(\epsilon)$
F	coefficient in Eq. (31)
g	acceleration due to gravity (m/s^2)
$g = y'(0)$	coefficient in the Taylor expansion of $y(\epsilon)$
G	coefficient in Eq. (31)
h	heat transfer coefficient ($W/(m^2 K)$)
H	length of the horizontal conic (m)
H	coefficient in Eq. (31)
I	current of the heater (A)
J	constant defined by integral (52) (dimensionless)
K	constant in the relation (26) (dimensionless)
$Nu = \frac{hR}{\lambda}, = \frac{hD}{\lambda}$	Nusselt number (dimensionless)
M	arbitrary point of the conical surface
p	pressure (N/m^2)
P	function defined by Eq. (46)
$r = \rho_0 K^{1/3}$	dimensionless radius coordinate (dimensionless)
R	radius of the cone (m)
Q	heat flow (W)
$Ra = \frac{g\beta\Delta TR^3}{va}, = \frac{g\beta\Delta TD^3}{va}$	Rayleigh number (dimensionless)
s	unit vector, tangent to the curve S (dimensionless)
S	curve, being the convective fluid flow streamlines on the lateral surface of the horizontal conic (dimensionless)
T	temperature (°C) or (K)
T_w	wall temperature (°C)
T_∞	bulk fluid temperature (°C)
ΔT	temperature difference (K)
U	voltage of the heater (V)
W	velocity (m/s)
x	coordinate (m)
X_i	constants in Eqs. (27)–(30) (dimensionless)
$y(\epsilon)$	dimensionless boundary layer thickness (dimensionless)
y	coordinate (m)
$Y = y(0)$	coefficient in the Taylor expansion of $y(\epsilon)$
z	coordinate (m)
$Z = Y^4$	function of the Y (dimensionless)

Greek symbols

α	base angle of the conic (deg)
β	average volumetric thermal expansion coefficient (1/K)
δ	boundary layer thickness (m)
ϵ	angle defined in Fig. 2 (deg)
ξ	distance between curves S (Fig. 5) (m)
λ	thermal conductivity of the fluid (W/(m K))
v	kinematic viscosity (m^2/s)
ρ	radius defined in Fig. 3 (m)
ρ_f	density of the fluid (kg/m^3)
σ	vector normal to the curve S (m)
τ	vector tangent to the curve S (m)
Θ	nondimensional temperature (dimensionless)
Σ	lateral surface of the conic

$$x^2 + y^2 - z^2 \cot^2(\alpha) = 0, \quad 0 \leqslant z \leqslant H \tag{1}$$

or by ρ, ε, z, where $x = \rho \sin(\epsilon)$, $y = \rho \cos(\epsilon)$ (Fig. 3). The base angle α is a parameter of the conical surface which varied from $\alpha = \pi/2$—horizontal cylinder to $\alpha = 0$—round vertical plate.

At arbitrary point M_i of the lateral conical surface Σ one may distinguish two tangent vectors $\bar{\tau}_\rho$ and $\bar{\tau}_\epsilon$ and normal $\bar{\sigma}$ to the surface.

$$\bar{\tau}_\rho = \frac{\partial \bar{r}}{\partial \rho}, \bar{\tau}_\epsilon = \frac{\partial \bar{r}}{\partial \epsilon} \quad \text{where } \bar{r} = (x, y, z) \in \Sigma, \tag{2}$$

$$\bar{\sigma} = \bar{\imath} \sin\alpha \sin\epsilon + \bar{\jmath} \sin\alpha \cos\epsilon - \bar{k} \cos\alpha. \tag{3}$$

Decomposition of the gravity with respect to these coordinates gives the normal component of gravity force $g_\sigma = g \sin\alpha \sin\epsilon$, $\bar{g} = (-g, 0, 0) = -\bar{\imath}g$.

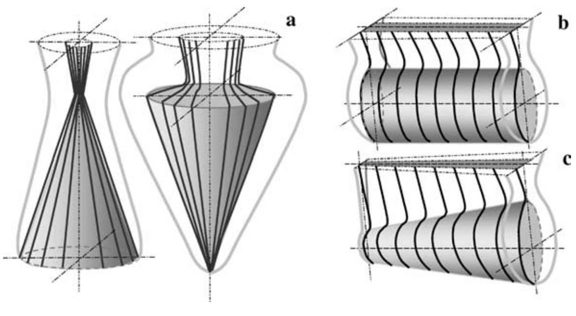

Fig. 1. Free convective fluid flow pattern described by boundary layer thickness (gray lines) and stream lines close heated surface and in a plume (black lines) for: (a) vertical cones, (b) horizontal cylinder and (c) horizontal conic.

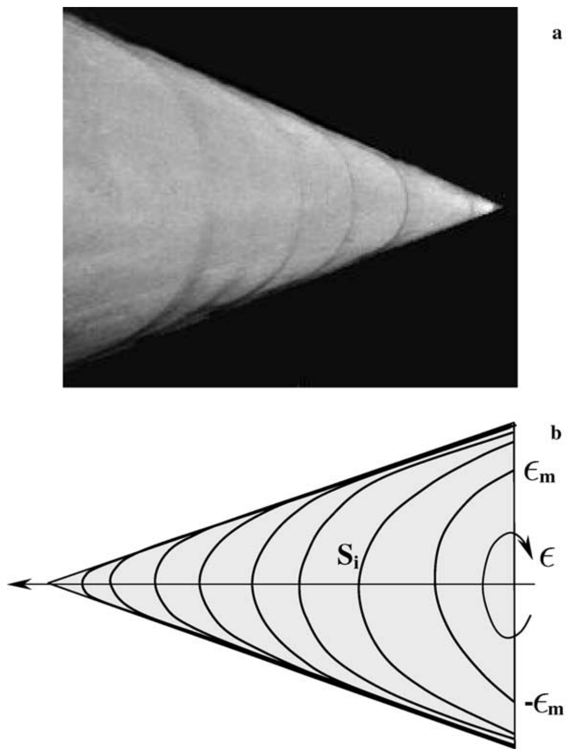

Fig. 2. Result of the visualization of the stream lines on the horizontal, isothermal conic transferred heat by free convection (a) and the model of the phenomenon described by curvilinear coordinate system $(\epsilon, \epsilon_{\rm m})$ with stream line curves S_i (b).

Let us now define a tangent component of the gravity. After normalization this component takes the form

$$\bar{s} = \frac{\bar{g} - (\bar{g}, \bar{\sigma})\bar{\sigma}}{g\sqrt{1 - \sin^2\alpha\sin^2\epsilon}} = \frac{-\bar{\imath}(1 - \sin^2\alpha\sin^2\epsilon) + \bar{j}\sin^2\alpha\sin\epsilon\cos\epsilon - \bar{k}\cos\alpha\sin\alpha\sin\epsilon}{\sqrt{1 - \sin^2\alpha\sin^2\epsilon}}. \quad (4)$$

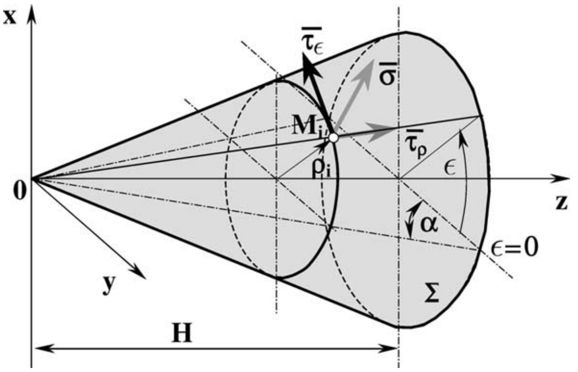

Fig. 3. Coordinate systems: Cartesian, curvilinear and local for the conic.

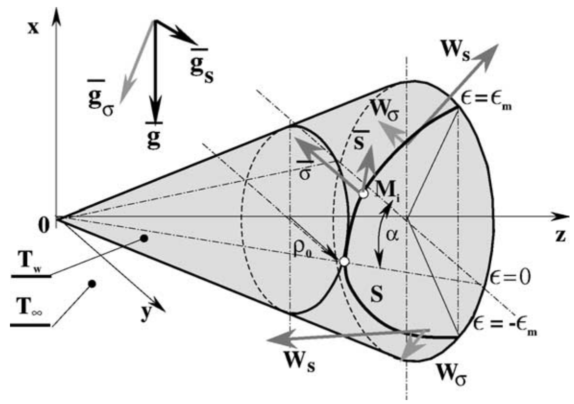

Fig. 4. The illustration of the curve S construction: it is defined as the vector $\bar{s}$ is tangent at every point of the curve S.

This unit vector $\bar{s}$ defines the curve S on the surface (Fig. 4). Hence the gravity component along $\bar{s} \times \bar{\sigma}$ is zero. That is why we solve the equations: Navier–Stokes, Fourier–Kirchhoff and continuity in these two characteristic directions $\bar{\sigma}$ and $\bar{s}$.

We use assumptions typical for natural convection [9]:

- fluid is incompressible and its flow is laminar,
- inertia forces are negligibly small in comparison with viscosity ones,
- the mass density $\rho_{\rm f}$, kinematic viscosity ν and volumetric expansion β in the boundary layer and undisturbed region (index ∞) are constant,
- tangent to the heated surface component of the velocity inside the boundary layer is significantly larger than normal one $W_s \gg W_\sigma$. By this assumption two marginal regions are excluded: the first where the boundary layer arises $\epsilon = -\epsilon_{\rm m}$ and the second where it is transferred into the free buoyant plum $\epsilon = \epsilon_{\rm m}$.
- temperature of the lateral conical surface $T_{\rm w}$ is constant,
- thicknesses of the thermal and hydraulic boundary layers are the same.

Finally the Navier–Stokes equations may be written

$$\nu\frac{\partial^2 W_s}{\partial\sigma^2} - g_s\beta(T - T_\infty) - \frac{1}{\rho_{\rm f}}\frac{\partial p}{\partial s} = 0, \quad (5)$$

$$-g_\sigma\beta(T - T_\infty) - \frac{1}{\rho_{\rm f}}\frac{\partial p}{\partial\sigma} = 0. \quad (6)$$

The coordinates σ and s are local ones along the vectors $\bar{\sigma}$ and $\bar{s}$.

We evaluate the normal and tangent components of gravity as

$$g_\sigma = \bar{\sigma}\cdot\bar{g} = -g\sin\alpha\sin\epsilon, \quad (7)$$

$$g_s = g\sqrt{1 - \sin^2\alpha\sin^2\epsilon}. \quad (8)$$

We assumed that relation for temperature distribution inside boundary layer can be used as solution of Fourier–Kirchhoff equation [12,13]

$$\Theta = \frac{T - T_\infty}{T_w - T_\infty} = \left(1 - \frac{\sigma}{\delta}\right)^2 \quad \text{or} \quad T - T_\infty = \Delta T\left(1 - \frac{\sigma}{\delta}\right)^2. \tag{9}$$

Plugging (7)–(9) into (5) and (6) gives

$$v\frac{\partial^2 W_s}{\partial \sigma^2} - g\beta\Delta T\left(1 - \frac{\sigma}{\delta}\right)^2 \sqrt{1 - \sin^2\alpha \cdot \sin\epsilon} - \frac{1}{\rho_f}\frac{\partial p}{\partial s} = 0. \tag{10}$$

$$-g\beta\Delta T \sin\alpha \sin\epsilon \left(1 - \frac{\sigma}{\delta}\right)^2 - \frac{1}{\rho_f}\frac{\partial p}{\partial \sigma} = 0. \tag{11}$$

Integration of Eq. (11) for the boundary condition $\sigma = \delta,\ p_\sigma = p_{\infty(\sigma \geqslant \delta)}$ gives a formula for the pressure distribution in a boundary layer directed tangent to the heating surface.

$$p_\sigma = -p_{\infty(\sigma \geqslant \delta)} - \rho_f g\beta\Delta T \sin\alpha \sin\epsilon \left(\sigma - \frac{\sigma^2}{\delta} + \frac{\sigma^3}{3\delta^2} - \frac{\delta}{3}\right). \tag{12}$$

Pressure $p_{\infty(\sigma \geqslant \delta)}$ represents the excess of pressure over the hydrostatic pressure, on the border of the boundary layer, which, as it was shown in the paper [11], is approximately constant.

Differentiating of Eq. (12) with respect to s along the curve S (for the complete derivation of the curve equation look [9]), parameterized by the minimum value ρ_0 of ρ

$$\rho = \rho_0 (\cos\epsilon)^{-\cos^2\alpha} \tag{13}$$

gives

$$\frac{\partial p}{\partial s} = -\rho_f g\beta\Delta T \sin\alpha \frac{(\cos\epsilon)^{\cos^2\alpha+1}}{\rho_0\sqrt{1 - \sin^2\epsilon \sin^2\alpha}}\left[\cos\epsilon\left(\sigma - \frac{\sigma^2}{\delta} + \frac{\sigma^3}{3\delta^2} - \frac{\delta}{3}\right) + \sin\epsilon\left(\frac{\sigma^2}{\delta} - \frac{2\sigma^3}{3\delta^3} - \frac{1}{3}\right)\frac{d\delta}{d\epsilon}\right]. \tag{14}$$

The parametrization of the curve S by ρ_0 in (13) is equivalent to the parametrization by

$$\epsilon_m = \arcsin \rho_0/R - \pi/2. \tag{15}$$

Plugging of the equality (14) into Eq. (10) leads to

$$v\frac{\partial^2 W_s}{\partial \sigma^2} + \rho_f g\beta\Delta T\left\{ -\left(1 - \frac{\sigma}{\delta}\right)^2 \sqrt{1 - \sin^2\alpha \sin\epsilon} + \frac{\sin\alpha(\cos\epsilon)^{\cos^2\alpha+1}\cos\epsilon}{\rho_0\sqrt{1 - \sin^2(\epsilon)\sin^2(\alpha)}}\left(\sigma - \frac{\sigma^2}{\delta} + \frac{\sigma^3}{3\delta^2} - \frac{\delta}{3}\right) + \sin\epsilon\left(\frac{\sigma^2}{\delta^2} - \frac{2\sigma^3}{3\delta^3} - \frac{1}{3}\right)\frac{d\delta}{d\epsilon}\right\} = 0. \tag{16}$$

A double integration of Eq. (16) for the boundary conditions $W_s = 0$ at $\sigma = 0, \delta$ and mean value evaluation through boundary layer gives:

$$\overline{W_s} = \frac{1}{\delta}\int_0^\delta W_s \, d\sigma = \frac{g\beta\Delta T\delta^2(\cos\epsilon)^{\cos^2\alpha+1}}{v\sqrt{1 - \sin^2\epsilon\sin^2\alpha}}\left(-\frac{1 - \sin^2\epsilon\sin^2\alpha}{40(\cos\epsilon)^{\cos^2\alpha+1}} + \frac{\sin\alpha\cos\epsilon\delta}{180\rho_0} + \frac{\sin\alpha\sin\epsilon}{72\rho_0}\frac{d\delta}{d\epsilon}\right) \tag{17}$$

The account the law of energy conservation

$$dQ = -\rho_f c_p\left(\overline{T - T_\infty}\right) d(A\overline{W_s}), \tag{18}$$

where A is the cross-section area of the boundary layer (see Fig. 5), after the substitution of the mean value of the temperature: $(\overline{T - T_\infty}) = \frac{\Delta T}{3}$ yields:

$$dQ = -\frac{1}{3}\rho_f c_p \Delta T \, d(A\overline{W_s}). \tag{19}$$

The heat flux described by Eq. (19) should be equal to the heat flux determined by the Newton's equation (20):

$$dQ = h\Delta T \, dA_k = -\lambda\left(\frac{\partial\Theta}{\partial\sigma}\right)_{\sigma=0}\Delta T \, dA_k, \tag{20}$$

where dA_k is the control surface of the conic (see Fig. 5).

The simplifying assumption of the temperature profile inside boundary layer (9), the dimensionless temperature gradient on the heated surface may be evaluated as

$$\left(\frac{\partial\Theta}{\partial\sigma}\right)_{\sigma=0} = -\frac{2}{\delta}$$

leads to

$$\frac{1}{6\lambda}\rho_f c_p \delta \, d\left(A\overline{W_\tau}\right) = -dA_k. \tag{21}$$

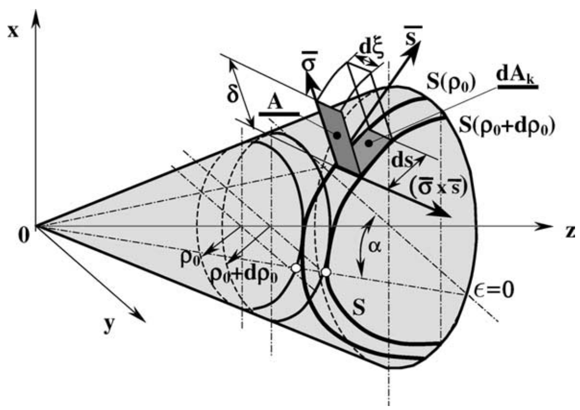

Fig. 5. Presentation of the elementary control surfaces: A and dA_k, defined by Eq. (22) and (23) for the coordinate curves $S(\rho_0)$ and $S(\rho_0 + d\rho_0)$ and the distance $d\xi$ between them.

The definitions of the cross-sectional area and the control surface A and dA_k are:

$$A = d\xi\delta = \frac{-(\cos\epsilon)^{1-\cos^2\alpha} d\rho_0\delta}{\cos\alpha\sqrt{1-\sin^2\alpha\sin^2\epsilon}}, \tag{22}$$

$$dA_k = d\xi\, d\tau = \frac{-(\cos\epsilon)^{-2\cdot\cos^2\alpha}\rho_0\, d\epsilon\, d\rho_0}{\cos\alpha}, \tag{23}$$

where

$$d\xi = \left|[\bar\sigma\times\bar\tau]\, d\bar r\right| = \frac{-(\cos\epsilon)^{1-\cos^2\alpha} d\rho_0}{\cos\alpha\sqrt{1-\sin^2\alpha\sin^2\epsilon}}. \tag{24}$$

Substituting Eqs. (17), (22) and (23) in Eq. (21) and evaluating the differentials one have

$$X_3(\delta\delta'' + 3\delta'^2) + (4X_2 + X_3')\delta\delta' + X_2'\delta^2 + 3X_1\rho_0\delta' + X_1'\rho_0\delta = \frac{\rho_0^2 X_4}{K\delta^3}, \tag{25}$$

where

$$K = \frac{Ra_R}{240R^3} = \frac{\rho_f c_p}{240\lambda}\frac{g\beta\Delta T}{v}, \quad Ra_R = \frac{g\beta\Delta T R^3}{va} \tag{26}$$

$$X_1 = -(\cos\epsilon)^{1-\cos^2\alpha}, \tag{27}$$

$$X_2 = \frac{2}{9}\frac{(\cos\epsilon)^{3+\cos^2\alpha}\sin\alpha}{(1-\sin^2\alpha\sin^2\epsilon)}, \tag{28}$$

$$X_2 = \frac{5}{9}\frac{(\cos\epsilon)^{2+\cos^2\alpha}\sin\alpha\sin\epsilon}{(1-\sin^2\alpha\sin^2\epsilon)}, \tag{29}$$

$$X_4 = (\cos\epsilon)^{-2\cos^2\alpha}. \tag{30}$$

Eq. (25) is the nonlinear ordinary differential equation to be considered as the basic one for free convection heat transfer along the arbitrary curve S which family covers the whole surface of isothermal horizontal conic.

3. Analytical approximate solution of the resulting equation

The resulting equation of the physical model could be solved by a simple numerical method. We, however, would apply analytical method to construct approximate formulas for the boundary layer thickness δ as a function of variables ϵ and ρ_0. Let us underline that our choice of the coordinate system allows to consider ρ_0 as a parameter. Rescaling in (25) $y(\epsilon) = \delta K^{1/3}$, $r = \rho_0 K^{1/3}$ yields:

$$y^4(\epsilon)E\frac{\partial\frac{\partial y(\epsilon)}{\partial\epsilon}}{\partial\epsilon} + 3y^3(\epsilon)E\frac{\partial y(\epsilon)^2}{\partial\epsilon} + y^3(\epsilon)\frac{\partial y(\epsilon)}{\partial\epsilon}G + y^5(\epsilon)H + y^4(\epsilon)F = r^2(1-\sin^2\alpha\sin^2\epsilon)\cos^{-2\cos^2\alpha}\epsilon. \tag{31}$$

where the coefficients are defined by

$$E = X_3(1-\sin^2\alpha\sin^2\epsilon) = \frac{5}{9}\cos^{2+\cos^2\alpha}\epsilon\sin\alpha\sin\epsilon, \tag{32}$$

$$\begin{aligned} G &= [y(4X_2 + X_3') + 3X_1 r](1-\sin^2\alpha\sin^2\epsilon) \\ &= 3(\cos^{1-\cos^2\alpha}\epsilon)r(\cos^2\epsilon + \cos^2\alpha - \cos^2\epsilon\cos^2\alpha) \\ &\quad + \frac{8}{9}(\cos^{3+\cos^2\alpha}\epsilon\sin\alpha)y(\epsilon), \end{aligned} \tag{33}$$

$$\begin{aligned} H &= X_2'(1-\sin^2\alpha\sin^2\epsilon) \\ &= \frac{2}{9}\frac{\sin\epsilon\sin\alpha}{\sin^2\alpha\sin^2\epsilon - 1}\cos^{2+\cos^2\alpha}\epsilon(\sin^2\epsilon\cos^4\alpha \\ &\quad + 3\cos^2\alpha + \cos^2\epsilon), \end{aligned} \tag{34}$$

$$\begin{aligned} F &= X_1' r(1-\sin^2\alpha\sin^2\epsilon) \\ &= \frac{r\sin^2\alpha(1-\sin^2\alpha\sin^2\epsilon)}{\cos^{\cos^2\alpha}\epsilon}\sin\epsilon. \end{aligned} \tag{35}$$

We consider an asymptotic solution as a power series in the vicinity of the point $\epsilon = 0$. This point is the singularity point of the equation: the coefficient by the second derivative is equal to zero when $\epsilon = 0$. The formal Taylor series expansion is

$$y(\epsilon) = \sum_{i=0}^{\infty} c_i\epsilon^i = Y + g\epsilon + f\epsilon^2/2 + \cdots$$

The coefficients of the expansion we determine directly from the differential equation (31) in the point $\epsilon = 0$. The equation gives connection of all coefficients with the first one $Y = y(0)$. This unique parameter is defined via the boundary condition $y(\epsilon_m) = 0$ in the point $\epsilon = \epsilon_m = \arccos(\rho_0/R)$.

Let us evaluate the first derivative of $y(\epsilon)$ at the point ($\epsilon = 0$). We start from Eq. (31) and solve it with respect to:

$$g = \left[\frac{\partial y(\epsilon)}{\partial\epsilon}\right]_{\epsilon=0} = \frac{9r^2}{(27r + 8(\sin\alpha)Y)Y^3}. \tag{36}$$

Next we should evaluate the second derivative of $y(\epsilon)$ at the point $\epsilon = 0$. For this aim we differentiate Eq. (36) and then solve the result with respect to:

$$\begin{aligned} f &= \left[\frac{\partial\frac{\partial y(\epsilon)}{\partial\epsilon}}{\partial\epsilon}\right]_{\epsilon=0} \\ &= -9\frac{423r^4(\sin\alpha)Y + 729r^2(r^3 + rY^8\sin^2\alpha + (\sin\alpha)Y^9)}{Y^7(27r + 13(\sin\alpha)Y)(27r + 8(\sin\alpha)Y)^2} \\ &\quad - 9\frac{16Y^9(\sin^2\alpha)(Y + r\sin\alpha)(4(\sin\alpha)Y + 27r)}{Y^7(27r + 13(\sin\alpha)Y)(27r + 8(\sin\alpha)Y)^2}. \end{aligned} \tag{37}$$

Details of the derivation of (36) and (37) are shown in papers [9,10].

Now we introduce the boundary condition at the edge of the cone, where the boundary layer arises

$$y(-\epsilon_m) = 0. \quad (38)$$

Here we restrict ourselves by parabolic approximation for the asymptotic expansion of the solution y of the differential equation of the boundary layer (31) in the form

$$y(\epsilon) = Y + g\epsilon + \frac{1}{2}f\epsilon^2. \quad (39)$$

Eq. (38) for the parameter Y is algebraic equation of high order, which has no explicit solution. So we expand the equation in Taylor series with respect to the variable $z = Y\sin\alpha/r$. In the region $(1/2)Y\sin\alpha \ll r$ one have in the first approximation

$$g = \frac{1}{3}\frac{r}{Y^3}, \quad (40)$$

$$f = -\frac{1}{3}\frac{r^2}{Y^3}. \quad (41)$$

After substitution of (40) and (41) into Eq. (39) it simplifies

$$Y^8 - \frac{1}{3}r\arccos(\rho_0/R)Y^4 - \frac{1}{6}r^2\arccos^2(\rho_0/R) = 0. \quad (42)$$

Introducing the new variable $Z = Y^4$ one goes to the second-order equation $Z^2 - (1/3)r\arccos(\rho_0/R)Z - (1/6)r^2\arccos^2(\rho_0/R) = 0$.

Solution has two roots, the first one is negative, hence non-physical and the second is positive, hence

$$Y = Z^{1/4} = \sqrt[4]{\frac{1}{2}\left(\frac{1}{6} + \frac{1}{6}\sqrt{7}\right)r[\pi - 2\arcsin(\rho_0/R)]}. \quad (43)$$

Finally the boundary layer thickness is

$$\delta(\epsilon) = \left(\frac{240\rho_0 R^3}{Ra}\right)^{1/4}\left(\sqrt[4]{\frac{1}{12}(1+\sqrt{7})[\pi - 2\arcsin(\rho_0/R)]} + \frac{\epsilon}{3\left(\frac{1}{12}(1+\sqrt{7})[\pi - 2\arcsin(\rho_0/R)]\right)^{3/4}} - \frac{\epsilon^2}{6\left(\frac{1}{12}(1+\sqrt{7})[\pi - 2\arcsin(\rho_0/R)]\right)^{7/4}}\right). \quad (44)$$

4. Integral heat transfer coefficient for practical applications

The solution (44) is local. However for practical applications one use the mean value of heat transfer coefficient, that is defined as the integral of the local value over the whole body surface.

From Eq. (20) it follows that the local value of heat transfer coefficient is

$$h = \frac{2\lambda}{\delta}. \quad (45)$$

Taking into account Eq. (15) the expression for boundary layer thickness (44) may be rewritten as

$$\delta(\epsilon) = R\left(\frac{240(\cos\epsilon_m)}{Ra}\right)^{1/4} a(\epsilon_m)\cdot P\left(\frac{\epsilon}{\epsilon_m}\right), \quad (46)$$

where

$$a(\epsilon_m) = \sqrt[4]{\frac{1}{6}(1+\sqrt{7})\epsilon_m},$$

$$P\left(\frac{\epsilon}{\epsilon_m}\right) = 1 + \frac{\epsilon}{\frac{1}{2}(1+\sqrt{7})\epsilon_m} - \frac{\epsilon^2}{\frac{1}{6}(1+\sqrt{7})^2\epsilon_m^2} = \left(1 + \frac{\epsilon}{3a^4} - \frac{\epsilon^2}{6a^8}\right).$$

Taking into account above given transformations of boundary layer thickness the local heat transfer coefficient h and it's dimensionless form Nu are:

$$Nu = \frac{h\cdot R}{\lambda} = \frac{2}{(\cos\epsilon_m)^{1/4}a(\epsilon_m)P\left(\frac{\epsilon}{\epsilon_m}\right)}\left(\frac{Ra}{240}\right)^{1/4}. \quad (47)$$

The mean value of Nusselt number for whole lateral surface of horizontal conic S can be expressed by the relation:

$$Nu_m = \frac{2}{S}\left(\frac{Ra}{240}\right)^{1/4}\int_0^{\pi/2}\int_{-\epsilon_m}^{\epsilon_m}\frac{1}{(\cos\epsilon_m)^{1/4}a(\epsilon_m)P\left(\frac{\epsilon}{\epsilon_m}\right)}\cdot dA_k. \quad (48)$$

Control surface of the cone dA_k is described with the use of ρ_0 (13) and $d\rho_0$ as the functions of ϵ_m (15):

$$dA_k = \cos\alpha\cdot(\cos\epsilon)^{-2\cdot\cos^2\alpha}\cdot R^2\cdot\sin\epsilon_m\cdot(\cos\epsilon_m)^{2\cos^2\alpha-1}\,d\epsilon_m\,d\epsilon. \quad (49)$$

Plugging (49) into (48) leads to final relation

$$Nu_m = C_R\cdot Ra^{1/4}, \quad (50)$$

where

$$C_R = \frac{2}{\pi}(\cos\alpha)^2\left(\frac{1}{240}\right)^{1/4}J \quad (51)$$

and

$$J = \int_0^{\pi/2}\left(\frac{\sin\epsilon_m(\cos\epsilon_m)^{2\cos^2\alpha-1}}{(\cos\epsilon_m)^{1/4}a(\epsilon_m)}\right)\times\left(\int_{-\epsilon_m}^{\epsilon_m}\frac{(\cos\epsilon)^{-2\cdot\cos^2\alpha}d\epsilon}{P\left(\frac{\epsilon}{\epsilon_m}\right)}\right)d\epsilon_m. \quad (52)$$

For practical application the obtained solution requires evaluation of the double integral over the surface J (52) which we made numerically. These calculations were performed for the following numbers of integration steps: $n = 300$, for the internal integral and $p = 150$, for the external one. The model of the boundary layer (44) is simplified, the direct corollary of this is the deviation of the asymptotic behavior of the local Nusselt number at the vicinity of the point $-\epsilon_m$, where the boundary layer arises. The integral (52) is hence divergent in this point. To regularize this discrepancy we integrate from the starting step -147 in all calculations. The results of the integral evaluations are: $J = 7.9359$, 10.337, 14.885 and 25.692 for $\alpha = 0$, 30°, 45° and 60°, respectively, and next: $C_R = 0.6478$, 0.6270, 0.6019 and 0.5194 for $\alpha = 0$, 30, 45 and 60 degrees for the radius of the cone base R as a characteristic linear dimension in Nusselt–Rayleigh relation (47) and (26). For comparison with experimental results elaborated with the use of the diameter $D = 2R$ as the characteristic linear dimension one can obtain: $C_D = \sqrt[4]{2} \cdot C_R = 0.763$, 0.746, 0.716 and 0.618 for $\alpha = 0$, 30°, 45° and 60° respectively.

5. Experimental apparatus

The experimental studies were performed in two set-ups using two fluids: distilled water and air. The both set-ups consist of a Plexiglas tank in a form of a rectangular prism of the volume 150 dm^3 for the water as a test fluid and 200 dm^3 for the air. The visualization of convective flow structures was performed in the water only while the quantitative experiments were made both in the water and in the air for four cones: $\alpha = 0$ (vertical round plate), $\pi/6$, $\pi/4$ and $\pi/3$. The investigated samples, excluding the vertical round plate ($\alpha = 0$), consist of two identical copper cones of the base diameter $D = 0.1$ m, that were joined in pairs according with Fig. 6 by the epoxy–resin (DISTAL). Each cone couple was suspended in a horizontal position by the use of nylon fishing twine of the diameter 0.1mm. In this way the heat losses through the base or supports were eliminated. We assumed that the heat losses through electric wiring were negligible small. The electric resistor as a source of heat was placed symmetrically inside the cavity of each sample. The concept of performed experimental measurement of a convective heat flux and the construction of the round vertical plate of the diameter $D = 0.07$ m were different in comparison with the cone case. The vertical plate of the sandwich layer construction consisted of two circular copper plates and epoxy–resin circular plate, of known thickness and heat conduction coefficient, between them was used in experiments. In this case the back heat losses flux was measured independently from temperature differences on both sides of epoxide plate with respect to Fourier equation. The thermal coefficient of conductivity for the laminate (copper–epoxy–resin–copper) was experimentally determined at a specially constructed stand. More

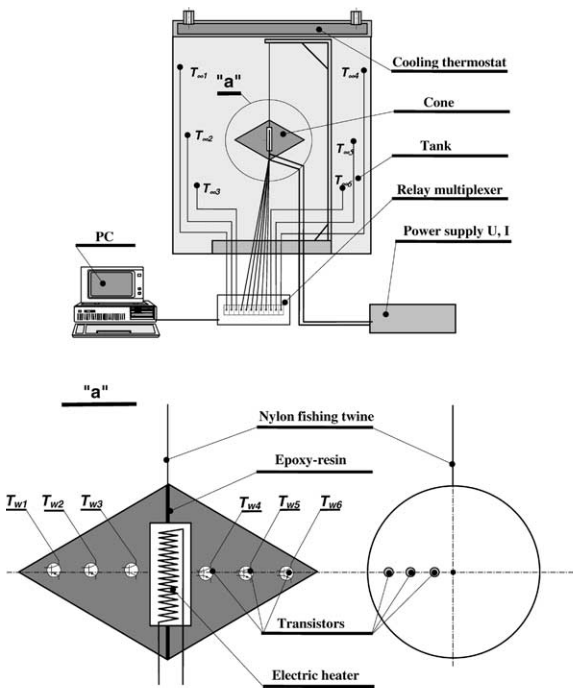

Fig. 6. Arrangement of the experimental apparatus and tested conic (enlarged detail "a").

details for this case one can found in our previous paper [14].

The surface of the cones were polished and next covered by chromium (electroplating) because the radiative heat losses have to be also taken into account in the experiments performed in the air. In calculations the emissive coefficient for the polished chromium was taken from the physical constants tables.

At the top of the tanks a cooler with thermostatic water of temperature equal to surrounding ±0.1 K was mounted. To measure the surface temperature T_w of the cones six transistors of the type BL 8473 were used. The transistors inserted through the opening of diameter 1 mm drilled from the base were glued by epoxy–resin to the surface of the cone. Also six transistors measured the fluid temperature in the undisturbed region T_∞. The temperatures of cone surfaces and fluids were calculated as a average value of all the particular transistors $T_{w,i}$ and $T_{\infty,i}$. The output signals from the transistors were processed by a computer program.

Experimental determination of Nusselt number was accomplished with an accuracy of ±6.6% for the water and ±5.6% for the air. The accuracy of Rayleigh numbers evaluation were ±4.3% (water) and ±2.1% (air).

6. Experimental results

Experimental results obtained for the water (dark points) and the air (white points) for the cones of the

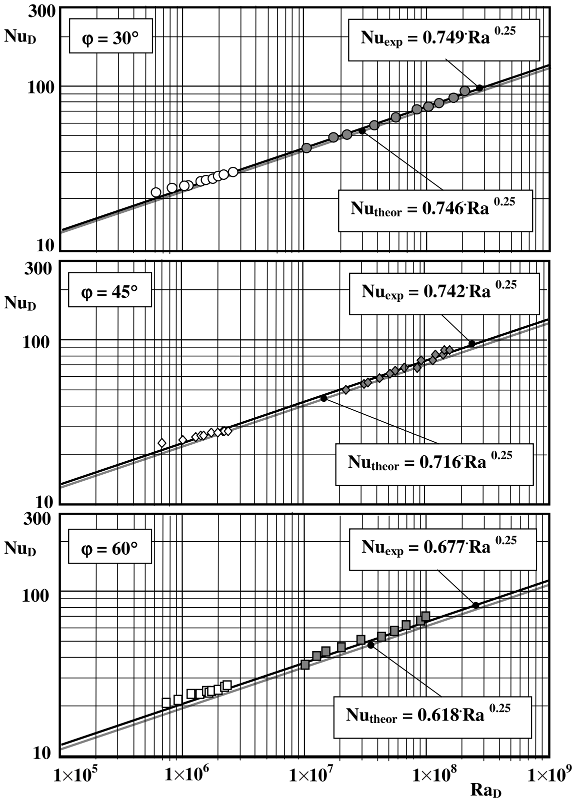

Fig. 7. Comparison of the theoretical results (brown lines) with the experiments (black line) performed in the air (white points) and the water (dark points).

base angle $\alpha = 30°$, 45° and 60° and analytical solution (grey lines) are presented in Fig. 7. By using the least square method the experimental data have been correlated by Nusselt–Rayleigh relation $Nu_D = C \cdot Ra_D^n$ for given value of the exponent $n = 1/4$. The results of these approximations together with the present solutions and literature data have been shown in Table 1. and in the frames in Fig. 7.

The Nusselt–Rayleigh formulas in Table 1 are valid for the range of the performed experimental studies: $6 \times 10^5 < Ra < 2 \times 10^8$ for air and $1 \times 10^7 < Ra < 2 \times 10^8$ for water which was obtained at wall-to-liquid temperature differences $9\ \mathrm{K} \leqslant \Delta T \leqslant 43$ K for air and $0.7\ \mathrm{K} \leqslant \Delta T \leqslant 9$ K for water.

The experimental results are presented once more in Fig. 8 in the form of $C = Nu_D/Ra_D^{1/4}$ vs. α so as the very point in the Fig. 8 is now the average of the results for all cases shown in frames in Fig. 7. These points together with literature data [14–17] were approximated by the second-order spline curve (grey line) described mathematically by the expression placed in the lower frame. The black line of Fig. 8 is also the second-order spline line but for the theoretical results, obtained by numerical evaluation of the integral (52).

As one can see the theoretical solution is convergent with experiments for vertical round plate $\alpha = 0°$ and for horizontal cone of the base angle $\alpha \leqslant 60°$. For the cones of the base angle α between 60° and 90° (horizontal cylinder) there is a divergences. It is a consequence of the use of the simplified asymptotic method of solution of Eq. (44).

The constants in Nusselt–Rayleigh experimental correlations recalculated for D as a characteristic linear dimension: $C_{exp} = 0.749$ for $\alpha = 30°$, $C_{exp} = 0.742$ for $\alpha = 45°$ and $C_{exp} = 0.677$ for $\alpha = 60°$, differs from the present solutions: $C_{theor} = 0.746$ for $\alpha = 30°$, $C_{theor} = 0.716$ for $\alpha = 45°$ and $C_{theor} = 0.618$ for $\alpha = 60°$ of about: +0.4% for $\alpha = 30°$, +3.5% for $\alpha = 45°$ and −8.2% and +8.7% for $\alpha = 60°$. This comparison can be regarded as a positive result of verification of obtained solution.

7. Conclusions

The results of the own experimental measurements and literature data of the free convective heat transfer in unlimited space of water and air from horizontal conics for the range of temperature differences $9\ \mathrm{K} \leqslant \Delta T \leqslant 43$ K for air and $0.7\ \mathrm{K} \leqslant \Delta T \leqslant 9$ K for water and Rayleigh numbers $6 \times 10^5 < Ra < 2 \times 10^8$ for air and $1 \times 10^7 < Ra < 2 \times 10^8$ for water are presented by the spline curve of the second-order for the base angle of the cone $0 \leqslant \alpha \leqslant 90$ deg. The spline function has the form: $C_{exp} = 0.672 + 3.959 \times 10^{-9}\alpha - 5.836 \times 10^{-5}\alpha^2$.

The theory elaborated in this paper is based on the typical for natural convection assumptions and cover all conditions described above. The resulting differential equation of the theory (25) is one-dimensional in the coordinate system that was specially constructed to account the geometry of horizontal cones and the gravitational field.

The obtained approximate solution describes convective heat transfer over horizontal isothermal conic in unlimited space. The structure of boundary layer that define the heat transfer and streamlines near the conical surface is described by the Taylor series near the points at $\epsilon = 0$. In this paper we present the solution based only on the first three terms of series. The approximate method of solution of the differential equation for boundary layer thickness in principle does not allow to obtained the correct description of the thickness in the vicinity of the starting point $\epsilon = -\epsilon_m$. The consequence of this is the divergence of the integral (52) that define the mean value of heat transfer coefficient. For all the cases of conic angles α we used universal approach of regularization of the integral.

Table 1
Comparison of own and literature theoretical and experimental results of free convective heat transfer from horizontal cones

Case	Criterial relations	Notes
$\alpha = 0°$ round vertical plate	$Nu = 0.763 \cdot Ra^{1/4}$	Present solution
	$Nu = 0.587 \cdot Ra^{1/4}$	Experiment of vertical round plate of diameter $D = 0.07$ m, water, [14]
	$Nu = 0.655 \cdot Ra^{1/4}$	Experiment of vertical round plate of diameter $D = 0.07$ m, air, [14]
	$Nu = 0.699 \cdot Ra^{1/4}$	Numerical calculations, FLUENT/UNS program for round plate and air, [14]
$\alpha = 30°$	$Nu = 0.746 \cdot Ra^{1/4}$	Present solution
	$Nu = 0.771 \cdot Ra^{1/4}$	Experiment in air for $D = 0.1$ m
	$Nu = 0.727 \cdot Ra^{1/4}$	Experiment in water for $D = 0.1$ m
	$Nu = 0.749 \cdot Ra^{1/4}$	Mean experimental correlation elaborated for air and water
$\alpha = 45°$	$Nu = 0.716 \cdot Ra^{1/4}$	Present solution
	$Nu = 0.745 \cdot Ra^{1/4}$	Experiment in air for $D = 0.1$ m
	$Nu = 0.738 \cdot Ra^{1/4}$	Experiment in water for $D = 0.1$ m
	$Nu = 0.742 \cdot Ra^{1/4}$	Mean experimental correlation elaborated for air and water
$\alpha = 60°$	$Nu = 0.618 \cdot Ra^{1/4}$	Present solution
	$Nu = 0.685 \cdot Ra^{1/4}$	Experiment in air for $D = 0.1$ m
	$Nu = 0.669 \cdot Ra^{1/4}$	Experiment in water for $D = 0.1$ m
	$Nu = 0.677 \cdot Ra^{1/4}$	Mean experimental correlation elaborated for air and water
$\alpha = 90°$ horizontal cylinder	$Nu = 0.480 \cdot Ra^{1/4}$	Experimental results of horizontal cylinders [15]
	$Nu = 0.518 \cdot Ra^{1/4}$	Experimental results of horizontal cylinders [16,17] for $Pr \to \infty$
	$Nu = 0.599 \cdot Ra^{1/4}$	Experimental results of horizontal cylinders [16,17] for $Pr \to 0$

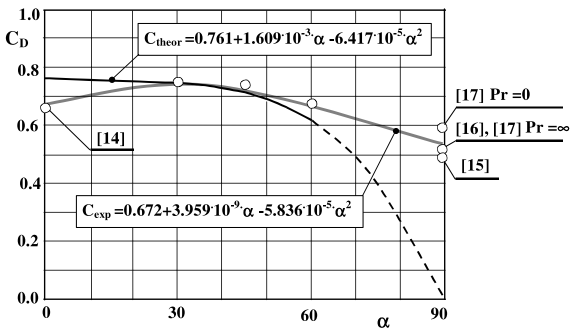

Fig. 8. Comparison of the own and literature experimental results described by $C_D = Nu_D/Ra_D^{1/4}$ (points and gray line) with analytical solution (black line).

Eventually the discrepancy in the result of calculations is connected with this. We plan to improve this point of the theory by matching of two asymptomatic for both singular points $\epsilon = 0$, $\epsilon = -\epsilon_m$. The algorithm described in the article allows to account arbitrary number of such terms in the Taylor series near the points at $\epsilon = 0$ and hence improve the heat transfer description.

Acknowledgements

This research was supported by Scientific Research of the Chemistry Faculty Gdańsk University of Technology.

References

[1] Md. Alamgir, Over-all heat transfer from vertical cones in laminar free convection an approximate method, J. Heat Transfer Trans. ASME 101 (1979) 174–176.
[2] W.M. Lewandowski, S. Szymański, P. Kubski, E. Radziemska, H. Bieszk, Natural convective heat transfer from isothermal conic, Int. J. Heat Mass Transfer 42 (1999) 1895–1907.
[3] W.M. Lewandowski, P. Kubski, S. Szymański, H. Bieszk, T. Wilczewski, E. Radziemska, T. Seramak, Natural convective heat transfer from conical surfaces, in: V UK National Conference on Heat Transfer, 1997.
[4] W.E. Stewart, Asymptotic calculation of free convection in laminar three-dimensional systems, Int. J. Heat Mass Transfer 14 (1971) 1013–1031.

[5] R.G. Hering, Laminar free convection from non isothermal cone at low Prandtl numbers, Int. J. Heat Mass Transfer 8 (1965) 1333–1337.
[6] P.H. Oosthuizen, E. Donaldson, Free convective heat transfer from vertical cones, J. Heat Transfer Transactions ASME (1972) 330–331.
[7] P.H. Oosthuizen, Free convective heat transfer from horizontal cones, J. Heat Transfer Transactions ASME (1973) 409–410.
[8] S.W. Churchill, Free convection around immersed bodies, 2.5 Single-Phase Convective Heat Transfer, in: 2.5 Single-Phase Convective Heat Transfer, Hemisphere Publishing Corporation, Washington, DC, 1983.
[9] S. Leble, W.M. Lewandowski, Analytical description of heat transfer by free convection from isothermal horizontal conic in unlimited space, MPS: Applied Mathematics/0301006 (2002).
[10] S. Leble, W.M. Lewandowski, A theoretical consideration of a free convective boundary layer on an isothermal horizontal conic, Appl. Math. Model. (2003).
[11] W.M. Lewandowski, Natural convection heat transfer from plates of finite dimensions, Int. J. Heat Mass Transfer 34 (3) (1991) 875–885.
[12] H.B. Squire, in: S. Goldstein (Ed.), Modern Developments in Fluid Dynamics, Clarendon Press, Oxford, 1938, or in Dover, New York, 1965.
[13] E.R.G. Eckert, Heat and Mass Transfer, McGraw-Hill Book Company, New York, 1959, pp. 312.
[14] W.M. Lewandowski, E. Radziemska, Heat transfer by free convection from an isothermal vertical round plate in unlimited space, Appl. Energy 68 (2001) 187–201.
[15] U.T. Morgan, The overall convective heat transfer from smooth circular cylinders, Adv. Heat Transfer 11 (1975) 199–264.
[16] S.W. Churchill, H.H.S. Chu, Correlating equations for laminar and turbulent free convection from a horizontal cylinder, Int. J. Heat Mass Transfer 18 (1975) 1049–1053.
[17] B. Gebhart, Natural convection flows and stability, Adv. Heat Transfer 9 (1973) 273–346.